Nonlinear Dynamics of Polymer Crystals

L.I. Manevitch [†] *, A.V. Savin [#]

[†] N.N. Semenov Institute of Chemical Physics, Russian Academy of Sciences, ul. Kosygina 4, 117977 Moscow, Russia

[#] State Institute of Physicotechnical Problems, ul. Prechistenka 13/7, 119034 Moscow, Russia

SUMMARY. Advances in the contemporary physics have led to the discovery of new elementary mechanisms that determine on the molecular level the progression of many physical processes in crystals and other ordered molecular structures. Early theoretical investigations of nonlinear dynamics of molecular chains [1-4] considered one-dimensional (spatially linear) models with the sign-positive anharmonism, which only took into account the longitudinal displacements of atoms (molecules) in the chain.

Introduction

Applications of the latter-day computational capabilities to the analysis of nonlinear dynamics of molecular systems permits going over from simple one-dimensional models to the more sophisticated two and three-dimensional models that better represent the actual geometric structure of a system. The most coherent and convenient objects in this respect are the zigzag molecular chains. The flat zigzag structure is much closer to reality than the one-dimensional anharmonic lattice. For example, we can consider a secondary structure, which brings a new factor into the dynamics of the system: the *geometrical anharmonism*. Even if all molecules are bound by harmonic forces, the geometry of the system gives rise to the effective negative anharmonism.

Many polymer macromolecules have the shape of flat zigzag. For example, the polyethylene (PE) macromolecule $(CH_2 —)_x$ in three dimensions has a stable two-dimensional *transzigzag* conformation. Consider this macromolecule chain represented schematically in Fig. 1. Here the interaction with the first neighbors takes place through deformation of valence bonds, and that with the second and third neighbors occurs through deformation of valence and torsional angles. As shown in [5, 6] in the approximation of infinitely rigid valence bonds the transition from the straight-line chain to the transzigzag conformation leads to a dramatic change in the

 CCC 1022-1360/00/$ 17.50+.50/0

type of soliton solutions. Instead of the compression solitons, the nonlinear elementary excitations come to be represented by the extension solitons that owe their existence to the geometric anharmonism.

The Hamiltonian of the chain may be written as

$$H = \sum_n \left\{ \frac{1}{2} M\left(\dot{u}_n^2 + \dot{v}_n^2\right) + V(\rho_n) + U(\theta_n) \right\}$$

Here the mass $M = 14 m_p$ (m_p is the mass of proton), $V(\rho_n) = D_0 \{1 - \exp[-\beta(\rho_n - \rho_0)]\}^2$ is the potential of the n-th valence bond, and $U(\theta_n) = \frac{1}{2}\varepsilon(\cos\theta_n - \cos\theta_0)^2$ is the potential of the n-th valence angle. According [7] $D_0 = 334.72$ kJ mol^{-1}, $\beta = 19.1$ nm^{-1}, and $\varepsilon = 130.122$ kJ mol^{-1}. In [8], a higher energy value was used, $\varepsilon = 529$ kJ mol^{-1}.

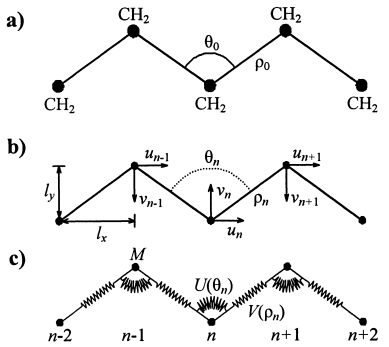

Fig. 1. a) Structure of polyethylene molecule $(CH_2)_\infty$; b) Selection of local coordinate systems; c) Mechanical model of macromolecule. In the equilibrium state $\rho_0 = 1.53$ Å, $\theta_0 = 113$ °.

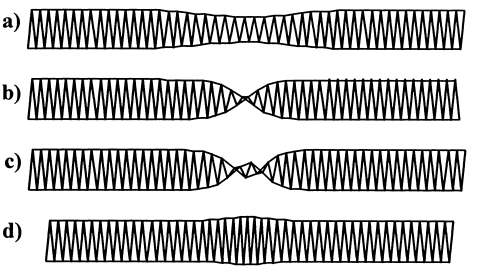

Fig. 2. Deformation of the transzigzag corresponding to an extension soliton of the first type, $s = 1.02$ (a), soliton of the second type, $s = 1.05$ (b), soliton of the third type, $s = 1.0738$, $\delta = 0.01929$ (c) and to a compression soliton, $s = 1.035$, $\delta = 0.07841$ (d).

We use a numerical technique of soliton analysis [9, 10], according to which for every value of the velocity c the soliton solution $u_n(t) = u(nl_x - ct)$, $v_n(t) = v(nl_x - ct)$, $n = 0, \pm 1, \pm 2, \ldots$, is sought as an extreme point of a certain functional.

Numerical analysis [11] indicates that the form of the soliton solution depends on the value of dimensionless parameter $\delta = \varepsilon \sin^2\theta_0 / 2D_0\beta^2\rho_0^2$ that characterizes the ratio between

physical and geometrical anharmonism. Physical anharmonism is due to the potential of the valence bond, whereas geometrical anharmonism is due to the potential of the valence angle. Geometrical anharmonism prevails at $\delta < 0.03556$, and physical one prevails at $\delta > 0.03556$.

With $\delta = 0.01928$ ($\varepsilon = 130.122$ kJ mol^{-1}), the system equations of motion

$$M\ddot{u}_n = -\frac{\partial H}{\partial u_n}, \quad M\ddot{v}_n = -\frac{\partial H}{\partial v_n}, \quad n = 0, \pm 1, \pm 2, \ldots \qquad (1)$$

admits three types of soliton solutions. The first type corresponds to a solitary wave of longitudinal extension of transzigzag with amplitude $A_n = \max_n v_n < l_y/2$ (the maximum value of the valence angle in the neighborhood of localization of soliton is $A_\theta < \pi$) and asymptotic behavior $w_n, v_n \to 0$ at $n \to -\infty$ (Fig. 2a) where $w_n = u_{n+1} - u_n$. The second type is a solitary wave of large-amplitude longitudinal extension of transzigzag (Fig. 2b) with the asymptotic behavior $w_n, v_n \to 0$ at $n \to -\infty$ and $w_n \to 0$, $v_n \to l_y$ at $n \to +\infty$. This solitary wave describes sequential unfolding of valence angle from one equilibrium value $\theta_n = \theta_0$ to the other $\theta_n = 2\pi - \theta_0$. As a result, the chain passes from one ground state $\{w_n \equiv 0, v_n \equiv 0\}$ to another $\{w_n \equiv 0, v_n \equiv l_y\}$. The third type corresponds to a solitary extension wave of transzigzag (Fig. 2c) with amplitude $l_y/2 < A_v < l_y$ ($\pi < A_\theta < 2\pi - \theta_0$) and asymptotic behavior $w_n, v_n \to 0$ at $n \to \infty$. This soliton is essentially a composite state of two opposite-sign solitons of the second type.

The energy E, the width D, and the overall longitudinal compression of the chain R as functions of the dimensionless soliton velocity $s = c/c_0$ are plotted in Fig. 3. The velocity of the long-wave longitudinal acoustic phonons (the speed of sound)

$$c_0 = 2\sqrt{K_2/M}\,\tan(\theta_0/2)/\sqrt{1 + 4\delta\tan(\theta_0/2)}$$

Solitons of the first type have supersonic spectrum of velocities $1 < s < s_1 = 1.020$. As the velocity of the soliton increases, the energy E and the overall compression of the chain R increase monotonically, and the width D of the soliton decreases. Solitons of the second type have the supersonic interval of admissible velocities $s_2 = 1.023 < s < s_3 = 1.062$. In this case, E, D, and R all decrease monotonically. Solitons of the third type only exist at one velocity value $s = s_4 = 1.074$.

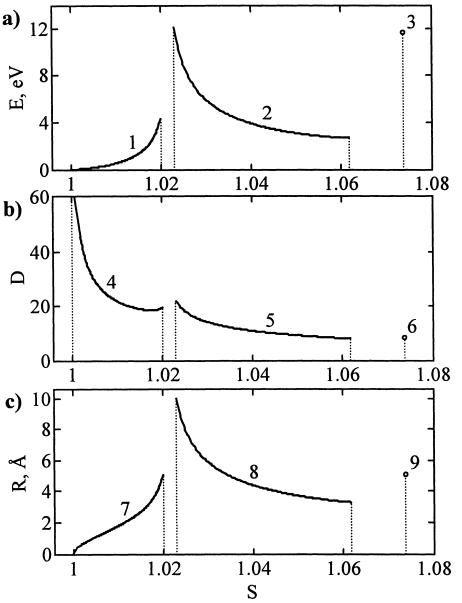

Fig. 3. Energy E (a), width D (b), and overall extension of the chain R (c) versus the velocity s of extension soliton of the transzigzag of the first (curves 1, 4, 7), second (curves 2, 5, 8) and third (curves 3, 6, 9) types.

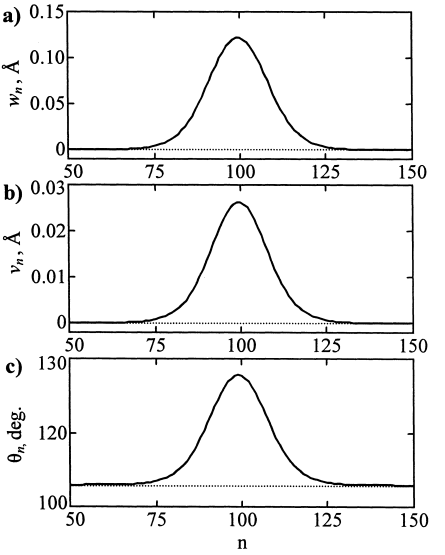

Fig. 4. Profile of an extension soliton of the first type with respect to components w_n (a), v_n (b), θ_n (c) at the initial time $t = 0$ and at the final time $t = 1613.8$ ps after passing 100 000 steps of the chain ($s = 1.015$).

The characteristic shape of a soliton of the first type is shown in Fig. 4. With respect to its components w_n, v_n, θ_n, the soliton has a characteristic bell-shaped profile of a solitary wave. In the region of localization of a soliton, the molecular chain exhibits longitudinal extension ($w_n > 0$) and transverse compression ($v_n > 0$). The valence angles increase, and the valent bonds stretch out. The existence of such solitons in the zigzag chain is due to the geometrical nonlinearity of the chain rather than to the proper (physical) anharmonism of the intermolecular potentials.

As the velocity increases, the energy and the amplitude of the soliton increase monotonically, and at $s = s_1$ attain their maximum values of $E_m = 4.6$ eV, $R_m = 5.3$ Å. The width of the soliton decreases, but always remains greater than 18 steps of the chain.

With the second value of the parameter $\delta = 0.078419$ ($\varepsilon = 529$ kJ mol^{-1}), the set of equations of motion (1) has a soliton solution corresponding to a solitary wave of longitudinal

compression of transzigzag (Fig. 2d). In the region of localization of soliton there is contraction of valence angles and bonds. The soliton has a finite velocity range $1 < s \leq 1.035$.

The velocity range of an acoustic soliton versus the dimensionless parameter δ is shown in Fig. 5. At $\delta < \delta_0 = 0.0356$, the soliton is a solitary extension wave, and at $\delta > \delta_0$ a solitary transzigzag compression wave. In a chain with $\delta = 0$ (approximation of infinitely rigid valent bond), the velocity range of the soliton is $1 < s < s_1 = 1.095$. As δ increases, the upper limit of the velocities s_1 decreases steady. At the threshold value $\delta = \delta_0$, the geometrical and physical anharmonisms cancel out, and the velocity range vanishes ($s_1 = 1$). A further increase of δ leads to monotone growth of the velocity range.

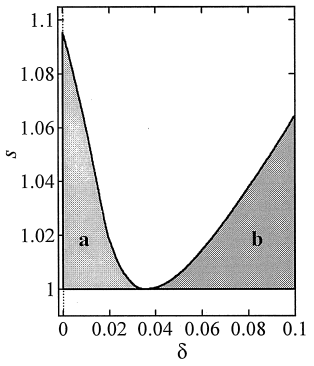

Fig. 5. Region of existence of an acoustic soliton of extension (a), and the region of existence of a soliton of transzigzag compression (b) in the space of dimensionless parameters δ and s.

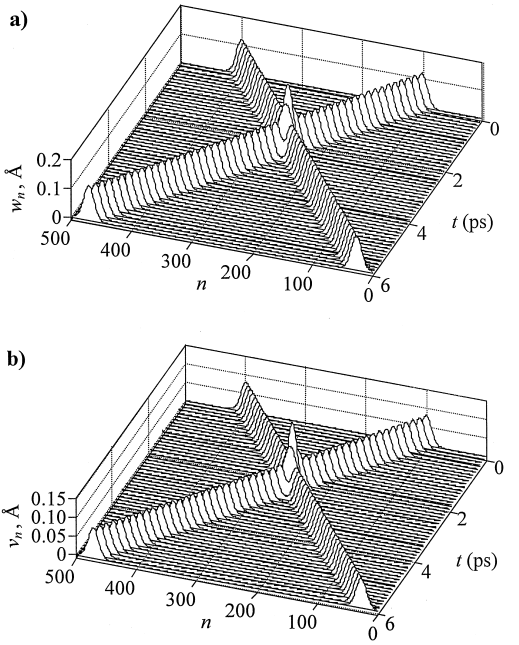

Fig. 6. Elastic collision of extension soliton of the first type in a cyclic chain of $N = 500$ sites: longitudinal displacements of steps of the chain versus time t (b); the same for transverse displacements.

Numerical simulation [10, 11] of the dynamics indicates that the soliton of the first type is dynamically stable at all values of the velocity $1 < s < s_1$. It moves at a constant speed, and completely retains its original shape. For example, with the initial dimensionless velocity

$s = 1.015$ ($c = 7906.85$ m/s, $\delta = 0.01929$), the soliton passed 99999.694 steps of the chain for 1613.8 ps, and had a final velocity of $s = 1.014995$ ($c = 7906.81$ m/s). As shown in Fig. 4, the final shape of the soliton is exactly the same as in the beginning. Solitons interact as elastic particles. Their collisions result in elastic reflection without emission of phonons or change of shape (Fig. 6). It is only near the limiting velocity s_1 that the interaction of solitons becomes inelastic: collision is accompanied by emission of phonons. Thus, near the speed of sound the extension solitons of the first type display definite particle-like properties. Solitons of the second type are unstable. When moving they emit phonons and soon perish. Solitons of the third type are stable at the velocity $s = s_4$. They move along the chain at a constant speed and retain their shape. Interaction between solitons of the third type is not elastic; collision between solitons leads to their destructions.

The above analysis of the transzigzag model indicates that isolated flat PE macromolecule may host dynamically stable extension solitons that display a relatively narrow spectrum of supersonic velocities. The existence of solitons is due to the geometrical anharmonism of the zigzag chain rather than to the physical anharmonism of potentials of intermolecular interaction.

Let us consider the problem of existence and stability of topological soliton in PE chain surrounded by immovable neighboring chains. Each polyethylene molecule in the crystal $(CH_2)_\infty$ is found in the *trans* conformation. Because in the studies of low-energetic dynamical processes in polyethylene, the motion of hydrogen atoms with respect to the main chain is not essential, the approximation of "united atoms" [12] can be used, so that we consider each CH_2 group as a single particle. In this approach only a monoclinic lattice can be stable [13]. Therefore we consider such a lattice with the periods $a' = \sqrt{a^2 + b^2}/2$, $b' = a$, $c' = c$ and parameters $a = 4.51$ Å, $b = 7.031$ Å, $c = 2\rho_0 \sin(\theta_0/2) = 2.552$ Å, providing the realistic density.

The corresponding structure of the crystal is presented in Fig. 7. All the macromolecules are situated in parallel planes. The structure of the crystal is completely determined by the zigzag angle and three parameters *a*, *b*, *c*. Let us consider an isolated molecule of the PE crystal. We choose the coordinate system in such a manner that the *n*-th unit CH_2 in the equilibrium state has coordinates

$$x_n^{(0)} = (-1)^n l_x/2, \quad y_n^{(0)} = 0, \quad z_n^{(0)} = nl_z$$

where $n = 0, \pm 1, \pm 2, \ldots$ is the number of units, and $l_x = \rho_0 \cos(\theta_0/2)$, $l_z = c/2 = \rho_0 \sin(\theta_0/2)$ are transversal and longitudinal constants of the transzigzag.

Next, we study the dynamics of only a central chain ($k = 0$) and take into account its interaction with the six neighboring chains ($k = 1, 2, \ldots, 6$) which are supposed to be immobile ("fixed neighbor" approximation). It is convenient to introduce the relative coordinates:

$$u_n = (-1)^{n+1}\left(x_n - x_n^{(0)}\right), \quad v_n = (-1)^{n+1} y_n, \quad w_n = z_n - z_n^{(0)}, \quad n = 0, \pm 1, \pm 2, \ldots$$

The local systems of coordinates are schematically shown in Fig. 7.

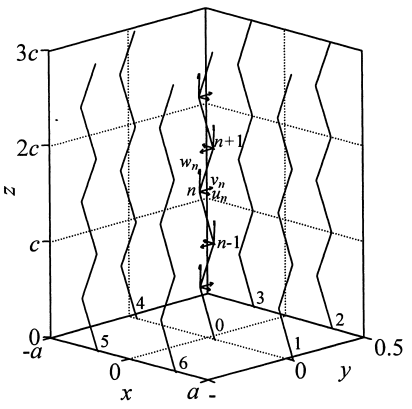

Fig. 7. Schematic representation of the crystalline PE. The central trans-zigzag backbone (curve 0) and the six neighbor chains (curves 1, 2, ..., 6) are shown. The local coordinates for the central chain are presented.

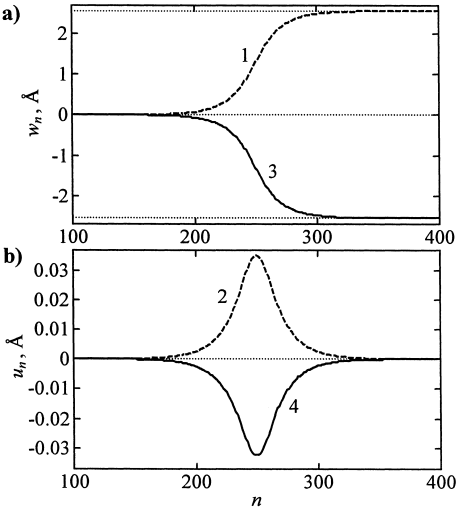

Fig. 8. The profiles of topological solitons with charge $\mathbf{q} = (1,0)$ (components w_n, u_n, curves 1, 2) after the passage of 10000 segments of the chain ($\tau = 40010.2$, $s = 0.2499$) and the profiles of the soliton with charge $\mathbf{q} = (-1,0)$ (curves 3, 4, $\tau = 40011$, $s = 0.2499$). Initial velocity is $s = 0.25$.

The Hamiltonian of the chain can be written as follows

$$H = \sum_n \left\{ \frac{1}{2} M\left(\dot{u}_n^2 + \dot{v}_n^2 + \dot{w}_n^2\right) + V(\rho_n) + U(\theta_n) + W(\delta_n) + Z(u_n, v_n, w_n) \right\} \qquad (2)$$

where the first term describes the kinetic energy of n-th unit, the second the deformation energy of the n-th valence bond, the third the deformation energy of the n-th valence angle,

the fourth the deformation energy of n-th torsional angle, and the last term the energy of interaction of the n-th unit with the six neighboring chains (substrate potential), $M = 14m_p$ is the mass of the united atom (m_p is the proton mass). The length of n-th valence bond is $\rho_n = \left(a_{n,1}^2 + a_{n,2}^2 + a_{n,3}^2\right)^{1/2}$, where $a_{n,1} = u_n + u_{n+1} - l_x$, $a_{n,2} = v_n + v_{n+1}$, $a_{n,3} = w_{n+1} - w_n + l_z$, the cosine of the n-th valence angle is $\cos(\theta_n) = (a_{n-1,1}a_{n,1} + a_{n-1,2}a_{n,2} - a_{n-1,3}a_{n,3})/\rho_{n-1}\rho_n$, and the cosine of the n-th torsional angle is $\cos(\delta_n) = (-b_{n,1}b_{n+1,1} - b_{n,2}b_{n+1,2} + b_{n,3}b_{n+1,3})/\beta_n\beta_{n+1}$, where $b_{n,1} = a_{n-1,2}a_{n,3} + a_{n,2}a_{n-1,3}$, $b_{n,2} = a_{n-1,1}a_{n,3} + a_{n,1}a_{n-1,3}$, $b_{n,3} = a_{n-1,2}a_{n,1} - a_{n,2}a_{n-1,1}$, $\beta_n = \left(b_{n,1}^2 + b_{n,2}^2 + b_{n,3}^2\right)^{1/2}$.

Following [7, 12], let us take the potential of the valence bond, valence angle, and torsional angle in the form $V(\rho_n) = D_0\{1 - \exp[-\alpha(\rho - \rho_0)]\}^2$, $U(\theta_n) = \frac{1}{2}\gamma(\cos\theta - \cos\theta_0)^2$, $W(\delta_n) = C_1 + C_2\cos\delta_n + C_3\cos 3\delta_n$ with the parameters $D_0 = 334.72$ kJ/mol, $a = 1.91$ Å^{-1}, $\gamma = 1330.122$ kJ/mol, $C_1 = 8.37$ kJ/mol, $C_2 = 1.675$ kJ/mol, $C_3 = 6.695$ kJ/mol.

The substrate potential $Z(u, v, w)$ in the Hamiltonian (2) can be presented [14] in the form

$$Z(u,v,w) = \varepsilon_w \sin^2(\pi w/l_z) + \frac{1}{2}K_u\left[1 + \varepsilon_u \sin^2(\pi w/l_z)\right]\left\{u - \frac{1}{2}l_x[1 - \cos(\pi w/l_z)]\right\}^2 + \frac{1}{2}K_v\left[1 + \varepsilon_v \sin^2(\pi w/l_z)\right]v^2$$

where ε_u = 0.0674265 kJ / mol, ε_v = 0.0418353 kJ / mol, ε_w = 0.1490124 kJ / mol, K_u = 2.169513 kJ/Å mol^2, and $K_v = 13.683865$ kJ/Å mol^2. The two-dimensional shape of this potential was first used [15] under the generalization of the Frenkel-Kontorova model for zigzag-like molecular chains.

The system equations of motion

$$M\ddot{u}_n = -\frac{\partial H}{\partial u_n},\quad M\ddot{v}_n = -\frac{\partial H}{\partial v_n},\quad M\ddot{w}_n = -\frac{\partial H}{\partial w_n},\quad n = 0, \pm 1, \pm 2, \ldots$$

admits three types of soliton solutions describing local topological defects in the crystal. They correspond, respectively, to (i) stretching or compression of the zigzag backbone by one lattice spacing (Fig. 8), (ii) stretching or compression over half-lattice spacing together with

twisting by 180 °C (Fig. 9), and (iii) pure twisting by 360 °C (Fig. 10). Let us determine the rotational angle of the n-th unit of the chain $\phi_n = \arg[l_x - u_n - u_{n+1} + i(v_n + v_{n+1})]$ where i is the imagine unity. The topological charge of the defect can be written as the two-dimensional vector $\mathbf{q} = (q_1, q_2)$, where $q_1 = (w_{+\infty} - w_{-\infty})/2l_x$, $q_2 = (\phi_{+\infty} - \phi_{-\infty})/2\pi$. Then the first type of defects has the topological charge $\mathbf{q} = (\pm 1, 0)$, the second one $\mathbf{q} = (0.5, \pm 0.5)$ $[\mathbf{q} = (-0.5, \pm 0.5)]$, and the third one $\mathbf{q} = (0, \pm 1)$.

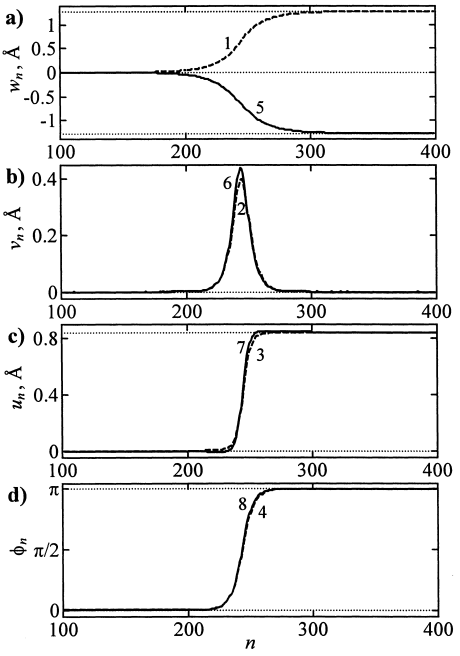

Fig. 9. The profiles of topological solitons with charge $\mathbf{q} = (0.5, 0.5)$ (components w_n, v_n, u_n, ϕ_n, curves 1, 2, 3, 4) after the passage of 10000 segments of the chain ($\tau = 40127.2$, $s = 0.2492$) and the profiles of the soliton with charge $\mathbf{q} = (-0.5, 0.5)$ (curves 5, 6, 7, 8, $\tau = 40174$, $s = 0.2488$). Initial velocity is $s = 0.25$.

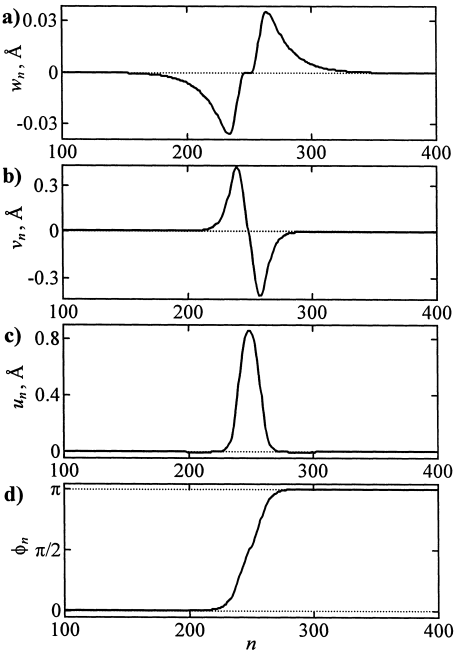

Fig. 10. The profiles of the topological soliton with charge $\mathbf{q} = (0,1)$ (components w_n, v_n, u_n, ϕ_n) after the passage of 10000 segments of the chain ($\tau = 40219.4$, $s = 0.2486$). Initial velocity is $s = 0.25$.

The existence of such solitons is caused by specific topology of the polyethylene crystal. All these solitons have the continuum spectra of velocities in the subsonic region. The most extended of them (40–50 chain segments) are solitons with topological charge $\mathbf{q} = (\pm 1, 0)$ (Fig. 8). The solitons with charge $\mathbf{q} = (0, \pm 1)$, have two times shorter length (Fig. 9). The

most massive quasiparticle (the rest mass is of 1.4 proton mass) is the soliton of torsion, the other solitons have the twice lighter mass (0.72–0.8 proton mass). The torsional solitons possess also the largest energy of formation of a pair of solitons of different signs (≥ 148 kJ/mol). The energy of formation of a pair of the stretching and compression solitons is ≥ kJ/mol, and the energy of formation of a pair of the stretching and torsional solitons and a pair of the compressional and torsional solitons is ≥ 81 kJ/mol. All the solitons have continuum spectra in the subsonic region. They [14] are dynamically stable and propagate with constant velocity retaining their profile – see figures 8, 9, 10.

The numerical modeling of the dynamics of the thermalized chain in crystalline PE has shown [14] that the thermal vibrations can lead to formation of only one type of local mobile defects, namely, the topological solitons corresponding to stretching (compression) of the zigzag chain by one half of the period of one chain accompanied by the torsion with 180 °C. The solitons with the pure stretching (compression) can be formed due to the interaction of the solitons of the former type only. Both these types of defects are topologically stable with respect to thermal vibrations of the chain. In a thermalized chain the defects can be formed as the pairs of the topological solitons of opposite signs and they propagate as Brownian particles. The solitons corresponding to the torsion of the chain by 360 °C are unstable with respect to thermal vibrations; they have a finite lifetime that exponentially decreases with the growth of temperature. The density of topological defects starts to grow sharply near the melting point that allows one to consider their accumulation as an initial mechanism of premelting the PE crystal.

This work was supported by the Russian Foundation of Basic Research (Grant No. 98-03-333-66a).

References

1. E. Fermi, J. Pasta, S. Ulam, in *Collected Works of Enrico Fermi* (Chicago: University of Chicago, 1965), Vol. II, p. 978
2. N.J. Zabusky, M.D. Kruskal, *Phys. Rev. Lett.* **15**, 241 (1965)
3. N.J. Zabusky, *Comput. Phys. Commun* **5**, 1 (1973)
4. M. Toda, *Phys. Rep.* **18**, 1 (1975)
5. L.I. Manevitch, N.L. Pahomova, V.V. Smirnov, S.V. Rjapusov, *Khim. Fiz.* **9** (4), 552 (1990)
6. L.I. Manevitch, S.V. Rjapusov, *Fiz. Tverd. Tela* (Leningrad) **34**, 1554 (1992)
7. B.G. Sumpter, D.W. Noid, G.L. Liang, B. Wunderlich, *Adv. Polymer Sci.* **116**, 29 (1994)

8. F. Zhang, *Phys. Rev E* **56**, 6077 (1997)
9. P.L. Christiansen, A.V. Savin, A.V. Zolotaryuk, *J. Comp. Phys.* **134**, 108 (1997)
10. L.I. Manevitch, A.V. Savin, *Phys. Rev. E* **55**, 4713 (1997)
11. A.V. Savin, L.I. Manevitch, P.L. Christiansen, A.V. Zolotaryuk, *Physics-Uspekhi* **42** (3) (1999)
12. D.W. Noid, B.G. Sumpter, B. Wunderlich, *Macromolecules* **24**, 4148 (1991)
13. M.K. Balabaev, O.V. Gendelman, L.I. Manevitch, M.A. Mazo, *Macromol. Sympos.* **106**, 31 (1996)
14. A.V. Savin, L.I. Manevitch, *Phys. Rev. B* **58**, 11386 (1998)
15. P.L. Christiansen, A.V. Savin, A.V. Zolotaryuk, *Phys. Rev. B* **54**, 12892 (1996)